Progressive Wavelet Packet Image Coding Using Compatible Zerotree Quantization *

Nasir Rajpoot[†] Francois Meyer[‡] Roland Wilson[§]
Ronald Coifman[¶]

e-mail: rajpoot-nasir@cs.yale.edu

Abstract

Wavelet packets are an effective representation tool for adaptive waveform analysis of a given signal. We first combine the wavelet packet representation with zerotree quantization for image coding. A general zerotree structure is defined which can adapt itself to any arbitrary wavelet packet basis. We then describe an efficient coding algorithm based on this structure. Finally, the hypothesis for prediction of coefficients from coarser scale to finer scale is tested and its effectiveness is compared with that of zerotree hypothesis for wavelet coefficients.

*This work was supported in part by DARPA/AFOSR under Grant F49620-97-1-0011.

[†]Department of Computer Science, University of Warwick, Coventry, UK and Department of Mathmatics, Yale University, New Haven, CT

[‡]Department of Computer Science, Yale University, New Haven, CT

[§]Department of Computer Science, University of Warwick, Coventry, UK

[¶]Department of Mathematics, Yale University, New Haven, CT

List of Figures

1 (*a*) A typical 3-level wavelet subband decomposition, (*b*) Compatible zerotrees for the subband families $\mathcal{H}$, $\mathcal{V}$, and $\mathcal{D}$ in (*a*). 5

2 (*a*) Wavelet packet subband decomposition with no parenting conflict (*b*) Wavelet packet subband decomposition with parenting conflict arising from the split of one of the children nodes of the vertical high-frequency subband LH_1. 7

3 (*a*) Sample segmentation in a 3-level wavelet packet decomposition, and (*b*) the parent-offspring dependencies for compatible zerotree originating from T_1. 8

4 The overall compatible zerotree structure comprising of the three primary compatible zerotrees T_1, T_2, and T_3; each node represents a whole wavelet packet subband, and the node radius is directly proportional to the support of wavelet packets at that transform level. 10

5 The overall compatible zerotree structure, after re-organization to resolve the parenting conflicts; the edge labels depict the rules used to generate the links between parent and the children nodes. 10

6 Plot of wavelet coefficients' amplitude versus coefficient indices for 5-level wavelet decomposition of 512×512 *Barbara* image; the subbands were arranged in an increasing frequency order. 13

7 Plot of wavelet coefficients' amplitude versus coefficient indices for 5-level wavelet decomposition of 512×512 *Barbara* image; the subbands were organized in compatible zerotrees with the help of rules mentioned in Section 3. 13

8 (*a*) Wavelet packet decomposition used for illustration of the compatible zerotree hypothesis for wavelet packets, (*b*) Compatible trees for the decomposition in *a*. 14

9 Plot of wavelet packet coefficients' amplitude versus coefficient indices for the wavelet packet decomposition shown in Figure 8(*a*) of the 512×512 *Barbara* image; the subbands were arranged in an increasing frequency order. 15
10 Plot of wavelet packet coefficients' amplitude versus coefficient indices for the wavelet packet decomposition shown in Figure 8(*a*) of the 512×512 *Barbara* image; the subbands were organized in compatible zerotrees with the help of rules mentioned in Section 3. 15
11 Zoomed sections of Figure 10 for the families T_1, T_2, and T_3 showing more sub-families within these compatible zerotrees. 16
12 Joint and conditional histograms for subband numbered 3 and its immediate children (binsize=80). 17
13 Joint and conditional histograms for subband numbered 4 and its immediate children (binsize=50). 18
14 Joint and conditional histograms for subband numbered 26 and its immediate children (binsize=100). 19
15 Joint and conditional histograms for subband numbered 43 and its immediate children (binsize=80). 20
16 Flowchart of the embedded wavelet packet image coding algorithm employing the compatible zerotree quantization strategy. 21
17 Portion of *Barbara* (table cloth) encoded at 0.25 bpp by (*a*) CZQ-WP and (*b*) SPIHT. 23
18 Wavelet packet basis selected for the 512×512 *Barbara* image. 24
19 Portion of *Fingerprints* (central spiral) encoded at 0.25 bpp by (*a*) CZQ-WP and (*b*) SPIHT. 25
20 Wavelet packet basis selected for the 512×512 *Fingerprints* image. . . . 26

1 Introduction

In recent years, there has been a surge of interest in wavelet transforms for image and video coding applications. This is mainly due to the nice localization properties of wavelets in both space and frequency. Wavelet coding techniques such as [14, 13] are known to perform well on images with relatively smooth regions. Recent work [9] on multi-layered representation of images for coding purposes uses the wavelet transform for encoding only smooth contents of the image. Wavelet packets [3] were developed in order to adapt the underlying basis to the contents of a signal (an image, in our case). The basic idea is to allow the non-octave subband decomposition to adaptively select the *best basis* for a particular signal. The nodes in a full subband tree (or short-term Fourier transform, namely STFT, tree) are pruned following a series of split/merge decisions using certain criterion (see [4] for entropy-based basis selection and [12] for optimizing the underlying basis using a rate-distortion framework). Results from various image coding schemes based on wavelet packets show that such methods are particularly good in encoding images with oscillatory patterns - a special form of *texture* containing rapid variations of the intensity. While wavelet packet bases are well adapted to the given signal (image), one apparently loses the parent-offspring dependencies, the *zerotrees* or the *spatial orientation trees*, as defined in [14, 13]. Zerotree quantization, proposed by Shapiro [14], is an effective way of exploiting the self-similarities among high-frequency subbands at various resolutions. The main thrust of this quantization strategy is in the prediction of corresponding wavelet coefficients in higher frequency subbands at the finer scales, by exploiting the parent-offspring dependencies. This prediction works well, in terms of efficiently coding the wavelet coefficients, due to the statistical characteristics of subbands at various resolutions, and due to the scale-invariance of edges in high frequency subbands of similar orientation. Various extensions of zerotree quantization, such as [6, 18], have been proposed since its introduction.

In this work, we address the following questions: *a*) Can the zerotree quanti-

zation strategy be applied to the wavelet packet transformed images? *b*) If so, how would the spatial orientation trees, or zerotrees, be defined in order to predict the insignificance of corresponding wavelet packets at a finer scale, given the wavelet packet at a coarser scale? The validity of former of these questions arises from the fact that one does not generally observe as much self-similarity among the wavelet packet subbands as among the wavelet subbands. We first provide an answer to the latter of these questions, assuming that the zerotree quantization can be applied to the wavelet packet decomposition of an image. This issue of wavelet packet zerotrees was addressed partially by Xiong et al. in [19]. In their work, however, the subband decomposition was restricted not to have a basis causing the *parenting conflict*, a problem explained in the next section. We present a solution to this problem and define a set of rules to construct the zerotree structure for an arbitrary wavelet packet geometry. This generalized zerotree structure is termed the *compatible zerotree* structure, for reasons mentioned in the next section, and provides a general quantization framework for efficiently encoding the wavelet packet coefficients. The answer to question *a*) becomes clear when we test the validity of this structure.

This paper is organized as follows. In the next section, a brief review of the wavelet packet transform and corresponding criteria used for the basis selection are presented. A general zerotree structure and the detailed algorithm for its construction are described in Section 3. The new zerotree quantization strategy is combined with the wavelet packet transform on the front end and an entropy coder on the back end. The image codec so obtained is explained in Section 4, and the experimental results are presented in Section 5. Finally, we conclude with a debate on the applicability of zerotree hypothesis for the wavelet packets and some suggestions for improvements in the codec's performance.

2 Wavelet Packet Transform

Block transform (such as DCT) coding methods (e.g.; the JPEG [10] image coding standard) produce undesirable blocking artifacts which are easily detectable by the human visual system (HVS). Local signal representation tools such as the short-term Fourier transform (STFT) and wavelet transform (WT) offer a solution to this problem by conjoining respectively frequency or scale to the position (time or space). The symmetry that exists among subbands of these transforms also provides a more efficient way of signal encoding in terms of coding gains. Practical coding schemes such as [1, 13, 14, 17] exploit these symmetry properties and have successfully exhibited their superiority over block transform coding methods. The artifacts caused by wavelet coding are known to be psychovisually tuned and thus are not so easily detectable even at medium bit rates. These methods, however, have a problem of their own at low bit rates. While they perform well on images containing smooth regions and edges, they perform poorly on images with oscillatory patterns (such as the well-known *Barbara* image). The quantization of many low-energy coefficients belonging to the high-frequency subbands causes artificial smooth regions (*smearing*) in the areas of image that contain rapid variations of intensities [8].

The need for an adaptive representation tool arises in order to tailor the underlying basis according to a given image instead of forcing a specific basis on images of all types. Generalized wavelet transforms such as wavelet packet transform [3] and multiresolution Fourier transform (MFT) [15] were developed to cater for this need. In this work, the former of these transforms is investigated using the zerotree quantization framework for image coding. Consider a 1-d discrete signal $\mathbf{x} = x_n$, $n = 0, 1, \ldots, N-1$. The wavelet packet coefficients are defined as follows:

$$\begin{aligned} w_{2n,j,l} &= \sum_k g_{k-2l}\, w_{n,j+1,k} \quad l = 0, 1, \ldots, N2^{j-J} \\ w_{2n+1,j,l} &= \sum_k h_{k-2l}\, w_{n,j+1,k} \quad l = 0, 1, \ldots, N2^{j-J} \\ w_{0,J,l} &= x_l \qquad\qquad\qquad\quad l = 0, 1, \ldots, N \end{aligned}$$

where $w_{n,j,l}$ is the transform coefficient corresponding to the wavelet packet basis which has relative support size 2^j, frequency $n2^j$ and is located at $l2^{-j}$, and $\{h_n\}$, $\{g_n\}$ are the lowpass and highpass filters respectively for a filter bank. The transform is invertible if appropriate dual filters $\{\tilde{h}_n\}$, $\{\tilde{g}_n\}$ are used on the synthesis side of this two-channel filter bank. Since this library of available basis functions provides an overcomplete description of the signal $\mathbf{x}$, a combination of basis vectors from this library is sought for which is well-suited to the signal and also forms an orthogonal basis. Although the overall variance is preserved by the decomposition of a given image (or subband) into low and high frequency subbands [1], it is the distribution of variance that determines if and how efficient the decomposition (split) is from a coding viewpoint. Various criteria have been used for computing the cost of a split (such as entropy as defined in [4], actual coding cost [8], and Lagrangian cost [12] function involving both rate and distortion) to decide whether such a split should be kept or the decomposed subbands should be merged. Coupling of such a criterion with a fast dynamic programming algorithm proposed first by Coifman and Wickerhauser [4] finds the *optimal* basis adapted to the image contents with respect to that particular criterion.

3 Zerotree Quantization for Wavelet Packets

Suppose that the best basis has been selected using any of the methods described in the previous section and zerotree quantization is to be used to encode the wavelet packet transform coefficients. The real issue is how to organize the spatial orientation trees so as to exploit the self-similarities, if any, among the wavelet packet subbands. The wavelet packet basis does not, in general, yield the parent-offspring relationships like those in the wavelet subbands. Due to the dyadic nature of wavelet subbands, the organization of parent-child relationships is quite straightforward. As shown in Figure 1(*a*), these dependencies are generated in such a manner that the whole subband decomposition is divided into three different types of subbands - horizontal, vertical, and diagonal. The four coeffi-

cients in a high-frequency subband are associated with a coeffi cient at same spatial location and belonging to subband of similar orientation at a coarser scale. Lewis and Knowles [7] hypothesized that in this tree-like structure, if the magnitude of a parent coeffi cient is below a given threshold, all of its children coeffi cients are most likely to follow this course too. This gave rise to the notion of *zerotrees*, a tree of insignifi cant or zero coeffi cients, which allow us to encode the whole lot of coeffi cients in such a tree using a single codeword.

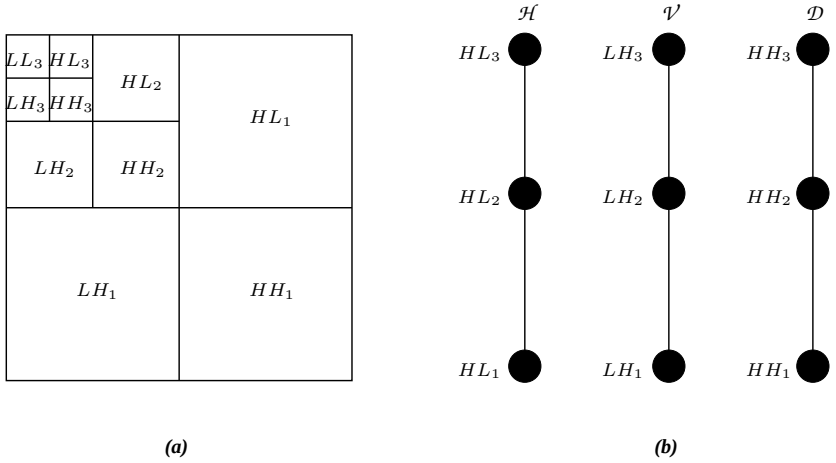

Figure 1: (*a*) A typical 3-level wavelet subband decomposition, (*b*) Compatible zerotrees for the subband families $\mathcal{H}$, $\mathcal{V}$, and $\mathcal{D}$ in (*a*).

We classify the subbands in a wavelet packet decomposition into three main categories, similar to three families of subbands in a wavelet decomposition, namely horizontal $\mathcal{H}$, vertical $\mathcal{V}$, and diagonal $\mathcal{D}$. We use the term *compatible zerotrees* to denote the trees of subbands having similar global orientation (ie, belonging to the same family). The adjective *compatible* originates from the fact that these trees are generated taking into account both the scale and orientation compatibility, as will be obivous from the rules defi ned for their construction. It is to be noted that the compatible zerotrees differ from the spatial orientation trees of [13] in the sense that the nodes of a compatible zerotree represent a full subband rather than one or

more transform coefficients. For instance, the compatible zerotrees associated with the three families $\mathcal{H}$, $\mathcal{V}$, and $\mathcal{D}$ of the wavelet decomposition, given in Figure 1(*a*), is shown in Figure 1(*b*). In case of a wavelet packet decomposition, the fact that the subbands of all the three families $\mathcal{H}$, $\mathcal{V}$, and $\mathcal{D}$ can be further decomposed, up to the coarsest scale, makes the construction of such a tree structure non-trivial. In the next section, we present a solution to the problem when a child node in the compatible zerotree is at a coarser scale than the parent node. The set of rules required to construct the compatible zerotrees is given in Section 3.2. The algorithms for the establishment of compatible zerotrees and the detection of zerotree root nodes in subbands belonging to such tree structures are provided in Section 3.3 and Section 3.4 respectively.

3.1 Parenting Conflict

As mentioned earlier, the high-frequency subbands in a wavelet packet decomposition can be further decomposed in order to adapt the basis to the image contents. In a pre-decomposed tree of one of these families of subbands ($\mathcal{H}$, $\mathcal{V}$, and $\mathcal{D}$), if a child node is decomposed into only four subbands of next coarser scale, the parent-offspring dependencies are easy to establish, as shown in Figure 2(*a*). However, if any of these four children nodes is decomposed any further, as shown in Figure 2(*b*), the resulting subbands $C_1,\ C_2,\ C_3$, and C_4 would be at a coarser scale than the parent node (subband) LH_2. This results in the association of each coefficient of such a child node to multiple parent coefficients, in the parent node, giving rise to a *parenting conflict*. In other words, there are four candidate coefficients in LH_2 claiming the parenthood of each of the four corresonding coefficients belonging to the children nodes C_i $(i = 1, \ldots, 4)$. In [19], the best basis was selected in such a way that whenever a conflict like this arises, the four children are merged so as to resolve the conflict. This suboptimal approach constrains selection of the best basis at the cost of a loss of freedom in adapting the wavelet packet basis to the contents of a given signal. In order to resolve the parenting conflict,

we suggest the following solution. Due to their orientation and scale compatibility with the subband LH_3, these children nodes C_i $(i = 1, \ldots, 4)$ can be moved up in the tree so that they are linked directly to LH_3, the root node of the compatible zerotree associated with the family $\mathcal{V}$ of subbands. This allows us to generate the compatible zerotree structure dynamically so that there is no restriction on selection of the wavelet packet basis.

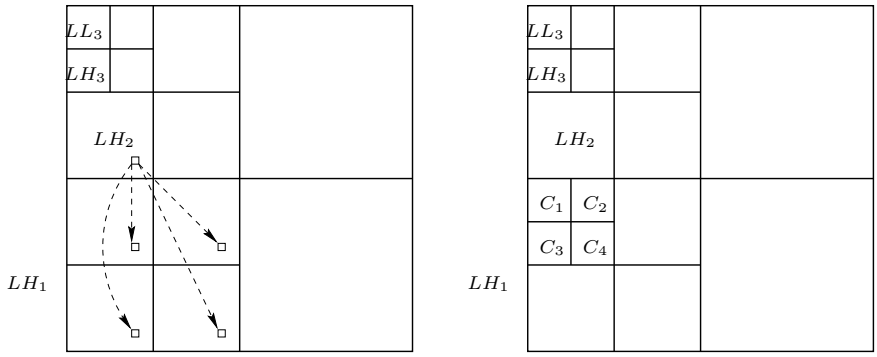

Figure 2: (*a*) Wavelet packet subband decomposition with no parenting conflict (*b*) Wavelet packet subband decomposition with parenting conflict arising from the split of one of the children nodes of the vertical high-frequency subband LH_1.

3.2 Rules

Once constructed for a given wavelet packet basis, the compatible zerotrees can be utilized to find the coefficients which are zerotree roots for various thresholds. In this section, a set of rules is defined so that the overall zerotree structure can be constructed for an arbitrary wavelet packet basis. The only *assumption* made is that the selected basis has the lowest frequency subband at the coarsest scale. This is a reasonable assumption which is based upon the fact that a significant amount of the signal energy is concentrated in the lowest frequency subband, which is most likely not to be merged by any of the tree pruning algorithms.

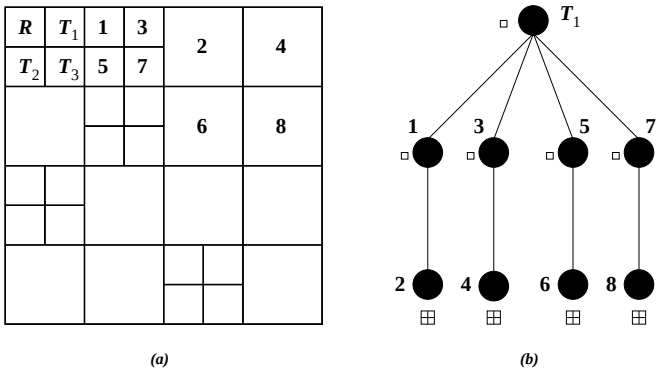

Figure 3: (*a*) Sample segmentation in a 3-level wavelet packet decomposition, and (*b*) the parent-offspring dependencies for compatible zerotree originating from T_1.

Consider the sample segmentation shown in Figure 3(*a*). Let R denote the node representing the lowest frequency subband situated in the top-left corner of a conventional subband decomposition. Then R represents the root node of overall compatible zerotree with T_1, T_2, and T_3 - which represent the coarsest scale high-frequency subbands - being its immediate children nodes, as shown in Figure 3(*a*). These children nodes are themselves roots of three compatible zerotrees corresponding to the families $\mathcal{H}$, $\mathcal{V}$, and $\mathcal{D}$ respectively. These compatible zerotrees are separately generated, only once for a given wavelet packet basis, in a recursive manner using the rules described below. In the description of these rules, "node X is followed by node Y" refers to the situation where node X is at a higher level (or coarser scale of pre-decomposed high-frequency subbands, as in a wavelet decomposition) than the node Y in the hierarchy of subbands in a given family tree.

a) If a node P at a coarser scale is followed only by a node C at the next finer scale (as in a wavelet transform), the node P is declared as a parent of C.
b) If a node P is followed by four nodes C_1, C_2, C_3, and C_4 (at the same scale), then P is declared to be the parent of all these four nodes.
c) If four subbands P_1, P_2, P_3, and P_4 at a coarser scale are followed by four subbands C_1, C_2, C_3, and C_4 at the next finer scale, then node P_i is declared

to be the parent of node C_i (for $i = 1, 2, 3, 4$).

d) If a node P is at a finer scale than four of its children, say C_1, C_2, C_3, and C_4, then P is disregarded as being the parent of all these nodes and all of them are moved in the tree under a node at the same or a coarser scale.

In a compatible zerotree, the parent-offspring relationships are established by looking at the scales of subband nodes in the tree. Unlike the compatible zerotrees for wavelet subbands (where each parent subband node is followed by exactly one child subband of similar orientation at the next finer scale and thus each coefficient of the parent node is associated with four coefficients of the child node at some spatial location), an intermediate node in a compatible zerotree, in general, can have more than one child node. What determines the parent-offpsring relationships between their coefficients is the difference in scale of the parent and child nodes. For instance, if both parent and the child nodes are at the same scale, each coefficient of the parent node will have exactly one offspring coefficient at same spatial location in the child node, whereas if the parent node is at the immediate coarser scale than the child node, then each coefficient of the parent node is associated with four coefficients at the same spatial location in the child node.

3.3 Compatible Zerotree Generation Algorithm

The construction of final compatible zerotrees proceeds in two steps. In the first step, the primary compatible zerotrees corresponding to the subband families $\mathcal{H}$, $\mathcal{V}$, and $\mathcal{D}$ are constructed using rules a, b, and c. In the second step, the overall tree is re-organized using rule d, in order to resolve any parenting conflicts. Let us consider the segmentation shown in Figure 3(*a*) to explain these rules. The primary compatible zerotrees T_1, T_2, and T_3 are generated, as shown in Figure 4, in the first step. The overall tree is re-organized (as shown in Figure 5) using rule *d* in order to resolve the parenting conflict under node P. This rule first identifies nodes with the parenting conflicts and when such nodes are found, the whole bunch (consisting of C_1, C_2, C_3, and C_4) is plucked from its current position in the tree. The algorithm

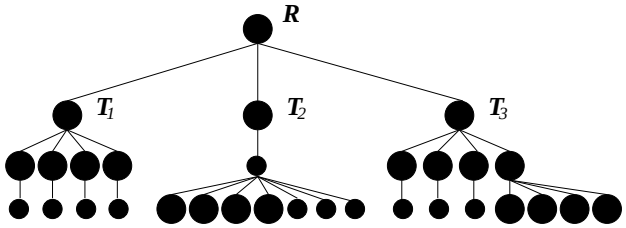

Figure 4: The overall compatible zerotree structure comprising of the three primary compatible zerotrees T_1, T_2, and T_3; each node represents a whole wavelet packet subband, and the node radius is directly proportional to the support of wavelet packets at that transform level.

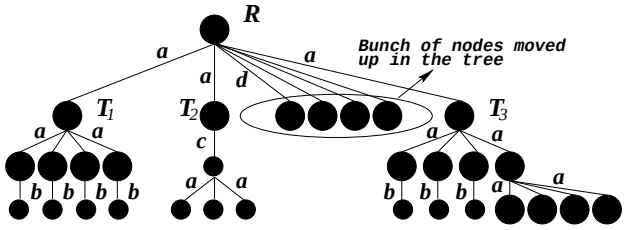

Figure 5: The overall compatible zerotree structure, after re-organization to resolve the parenting conflicts; the edge labels depict the rules used to generate the links between parent and the children nodes.

then climbs up the tree to look for an appropriate node, a compatible ancestor at the nearest scale and having the nearest orientation, and glues the bunch under this newly found compatible parent. The parent-offspring dependencies for the primary compatible zerotree T_1 are shown in Figure 3(*b*). The pseudocode of an algorithm for the generation of compatible zerotrees is given in the Appendix A.

Given an arbitrarily segmented wavelet packet basis, compatible zerotrees are constructed using the algorithm described above. In order to be able to make predictions for wavelet packet coeffi cients at fi ner scale subbands, the *compatible zerotree hypothesis* is defi ned as follows: If a wavelet packet coeffi cient of a node from the compatible zerotree is insignifi cant, it is more likely that the wavelet packet coeffi cients at similar spatial locations in all the descendent nodes of the

same compatible zerotree will be insignificant as well.

3.4 Utilizing the Compatible Zerotrees

The compatible zerotrees provide us a convenient way of making predictions about the insignificance of corresponding coefficients in the children nodes, given the significance of a coefficient belonging to the parent node. It is to be noted here that the compatible zerotrees are utilized for the detection of coefficients which are roots of the zerotrees. The encoding of zerotree codewords and information related to the significance of coefficients with respect to a threshold value follows the detection. Details of the algorithms used for the detection of zerotree root coefficients in each of the three primary compatible zerotrees and for the encoding are provided in Section 4.

3.5 Validating the Compatible Tree Organization

The success of compatible zerotree hypothesis for wavelet packets, as defined in Section 3.3, needs to be tested, and we employ two empirical ways of doing so. First, the amplitude of transform coefficients is plotted for all the subbands organized both in the ordinary increasing frequency order and in the compatible zerotrees. Consider the plots of wavelet coefficients' amplitude against the coefficient indices for a 5-level wavelet decomposition of the 512×512 *Barbara* image, as shown in Figures 6 and 7. The amplitude axis in both plots was restricted to ± 1000 to facilitate the display of smaller coefficients. While the subbands were arranged in an increasing frequency order for the plot in Figure 6, the plot in Figure 7 refers to the subbands as organized in the compatible zerotrees. Similar plots of wavelet packet coefficients' amplitudes against the coefficient indices for the same image using the basis geometry shown in Figure 8(*a*) (the corresponding compatible zerotrees are also shown in the Figure 8(*b*) with a numbering generated in a recursive manner) are given in Figures 9 and 10. In all plots corresponding to the subbands organized in the compatible zerotrees, three families of primary compatible zerotrees T_1, T_2, and T_3 are clearly visible showing that the new arrangement

is successful in isolating the coefficients of similar orientation in a hierarchy to be used for prediction in a top-down order. Zoomed plots of these families, as shown in Figure 11, exhibit more sub-families organized within these compatible zerotrees.

An alternate approach to test the success of compatible zerotree hypothesis is to actually compute the conditional probability $p(x|y)$ of the significance of a child coefficient x given the significance of its parent coefficient y for a specific threshold value. We plotted both joint and the conditional histograms to verify how successfully the prediction for insignificance of a coefficient in a child subband can be made given the insignificance of its parent coefficient. The joint and conditional histograms for some parent subbands and their immediate children using the subband decomposition of Figure 8(*a*) for *Barbara* are shown in Figures 12, 13, 14, and 15. The concentration of these histograms in the low-significance range of children coefficients throughout the range of parent coefficients is an encouraging evidence for the organization of these subbands in a compatible tree order. As is clear from the equation

$$H(X|Y) = H(X) - I(X,Y),$$

encoding the grouped significance information is more efficient than just encoding the individual coefficients' significance, if the mutual information $I(X,Y)$ - or the Kullback-Leibler divergence between the joint pdf $p(x,y)$ and the product pdf $p(x)p(y)$ [5] - is greater than zero. The success of compatible zerotree hypothesis, and thus the performance of zerotree encoding, depends largely upon $I(X,Y)$ for a given image, the basis used for its representation, and a specific threshold value. Larger the value of this measure, more successful the compatible zerotree hypothesis is going to be and thus more efficient the encoding is. Given basis $\mathcal{B}$ for an image, this value determines whether or not the basis $\mathcal{B}$ would be *friendly* to the zerotree quantization strategy.

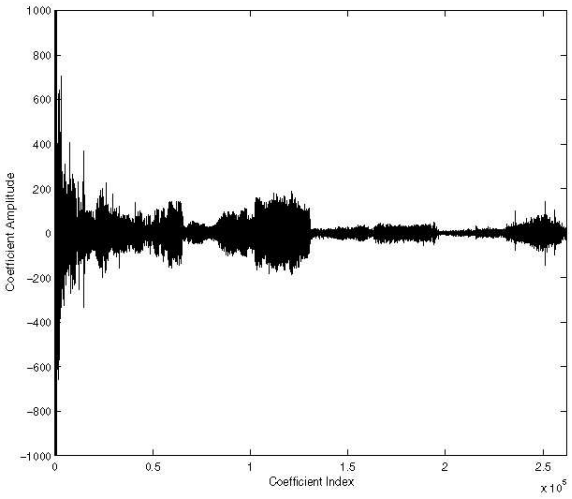

Figure 6: Plot of wavelet coefficients' amplitude versus coefficient indices for 5-level wavelet decomposition of 512×512 *Barbara* image; the subbands were arranged in an increasing frequency order.

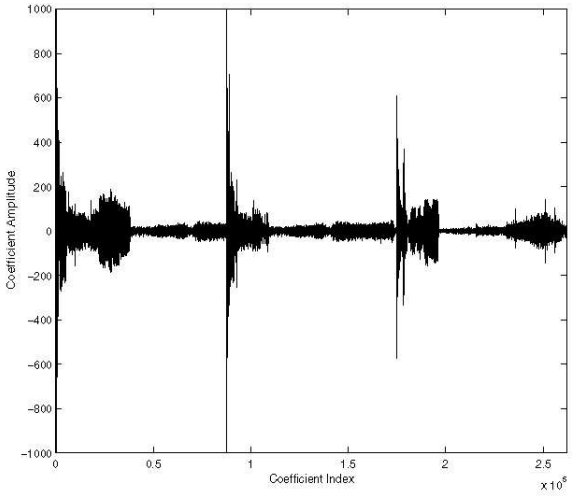

Figure 7: Plot of wavelet coefficients' amplitude versus coefficient indices for 5-level wavelet decomposition of 512×512 *Barbara* image; the subbands were organized in compatible zerotrees with the help of rules mentioned in Section 3.

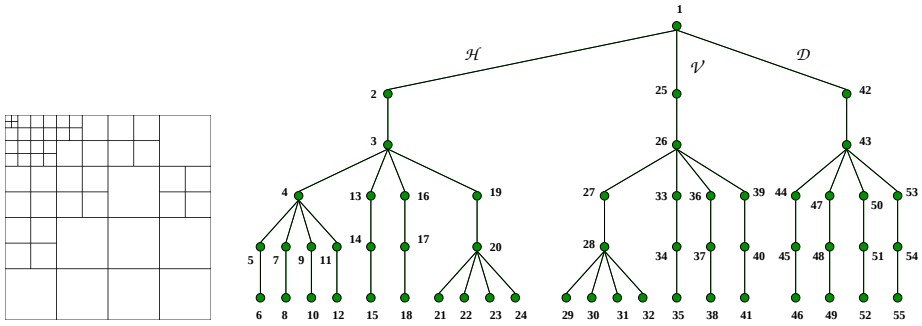

Figure 8: (*a*) Wavelet packet decomposition used for illustration of the compatible zerotree hypothesis for wavelet packets, (*b*) Compatible trees for the decomposition in *a*.

4 The Coder Algorithm

Once the compatible zerotrees have been generated, based upon knowledge of the best basis, the coding is performed by successively encoding the significance information about the coefficients, as they appear in the subbands in increasing frequency order, and the refinement information until the bit budget is expired. Detailed flowchart of the coder algorithm is given in Figure 16. Our algorithm requires only one list of detected coefficients (LDC) to be maintained, similar to [11], as opposed to two (or three) lists kept by the EZW (or SPIHT). The decoder first reads geometry of the best basis and generates the compatible zerotrees. It then proceeds by entropy decoding and interpreting the codewords until the bit budget is expired. The decoder is also capable of generating an approximation to the original image at any given bit rate or quality (as long as the minimum required bits are available for doing so.)

5 Experiments and Conclusions

The idea of compatible zerotree quantization was combined with the wavelet packet transform for progressive image coding and its performance was tested for two standard 8-bit grayscale 512×512 images containing oscillatory patterns us-

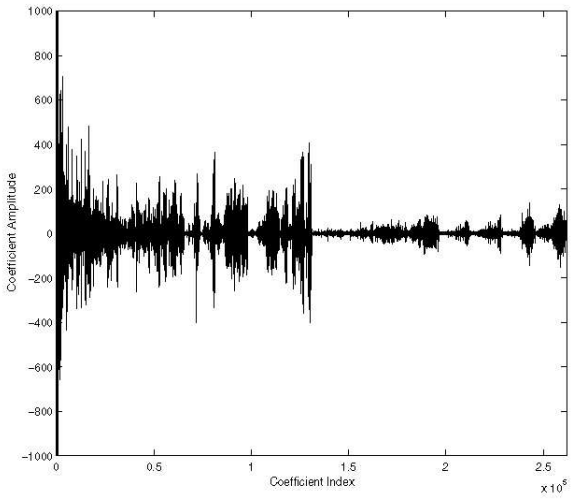

Figure 9: Plot of wavelet packet coefficients' amplitude versus coefficient indices for the wavelet packet decomposition shown in Figure 8(*a*) of the 512×512 *Barbara* image; the subbands were arranged in an increasing frequency order.

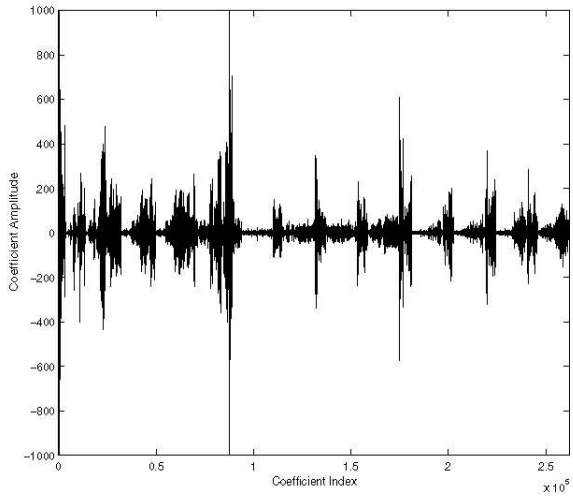

Figure 10: Plot of wavelet packet coefficients' amplitude versus coefficient indices for the wavelet packet decomposition shown in Figure 8(*a*) of the 512×512 *Barbara* image; the subbands were organized in compatible zerotrees with the help of rules mentioned in Section 3.

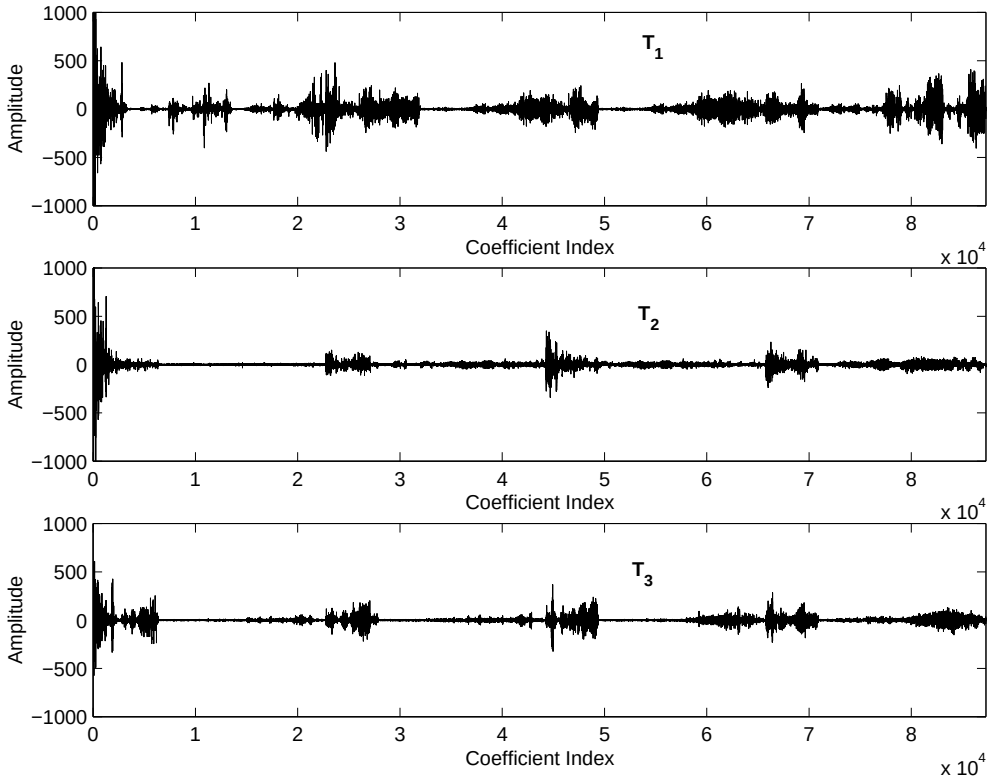

Figure 11: Zoomed sections of Figure 10 for the families T_1, T_2, and T_3 showing more sub-families within these compatible zerotrees.

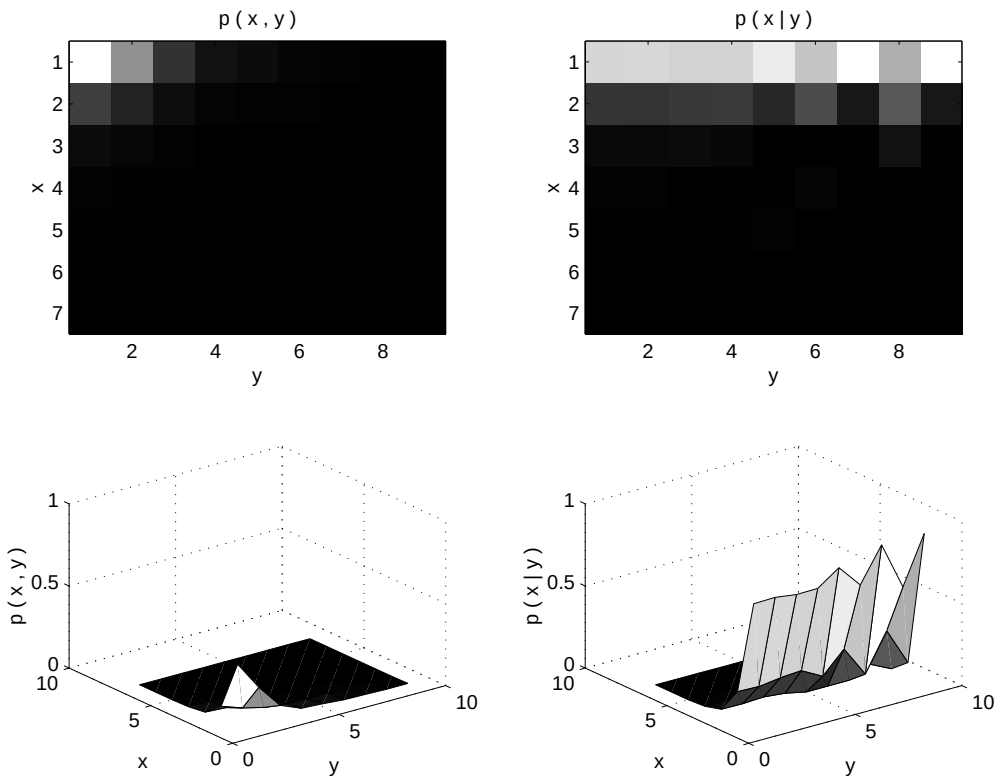

Figure 12: Joint and conditional histograms for subband numbered 3 and its immediate children (binsize=80).

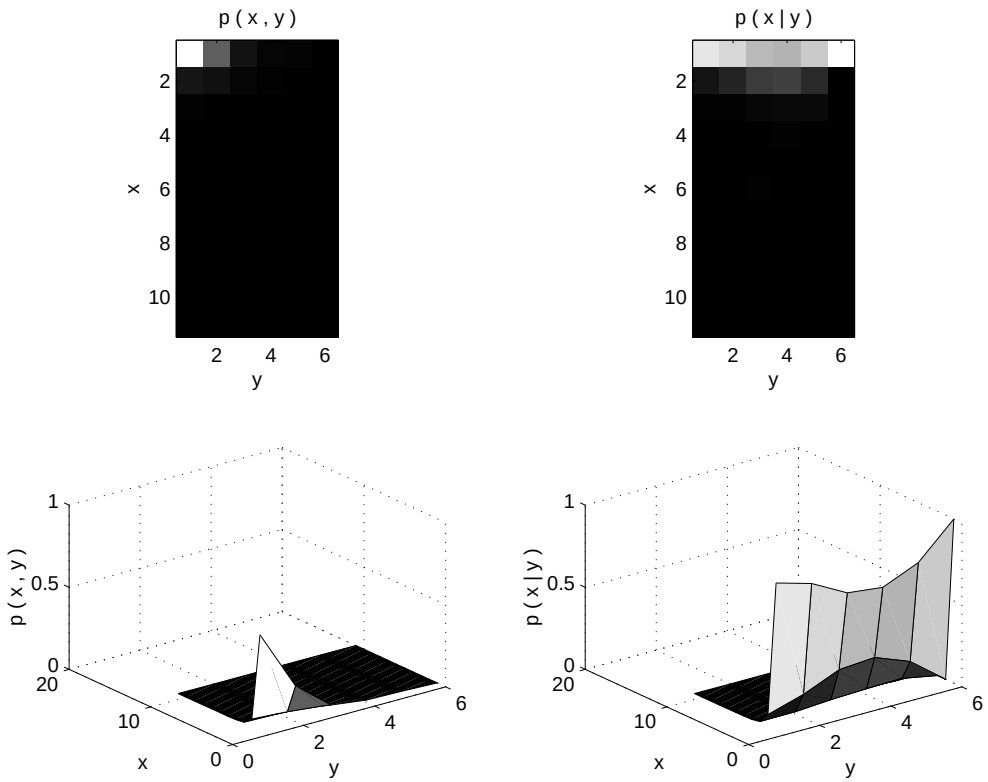

Figure 13: Joint and conditional histograms for subband numbered 4 and its immediate children (binsize=50).

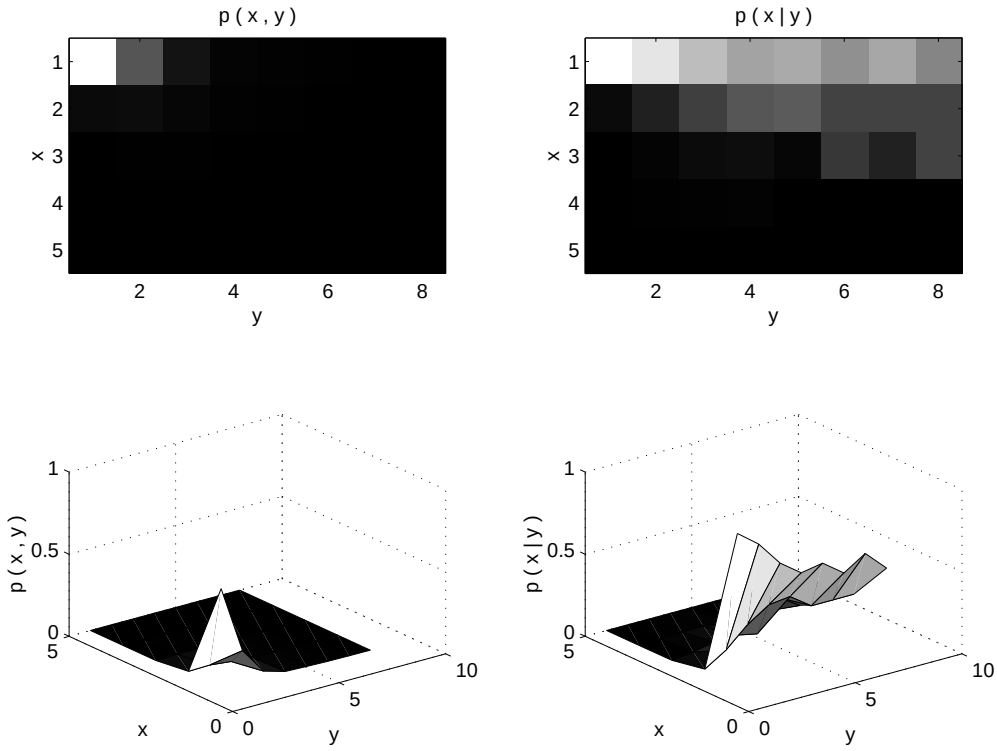

Figure 14: Joint and conditional histograms for subband numbered 26 and its immediate children (binsize=100).

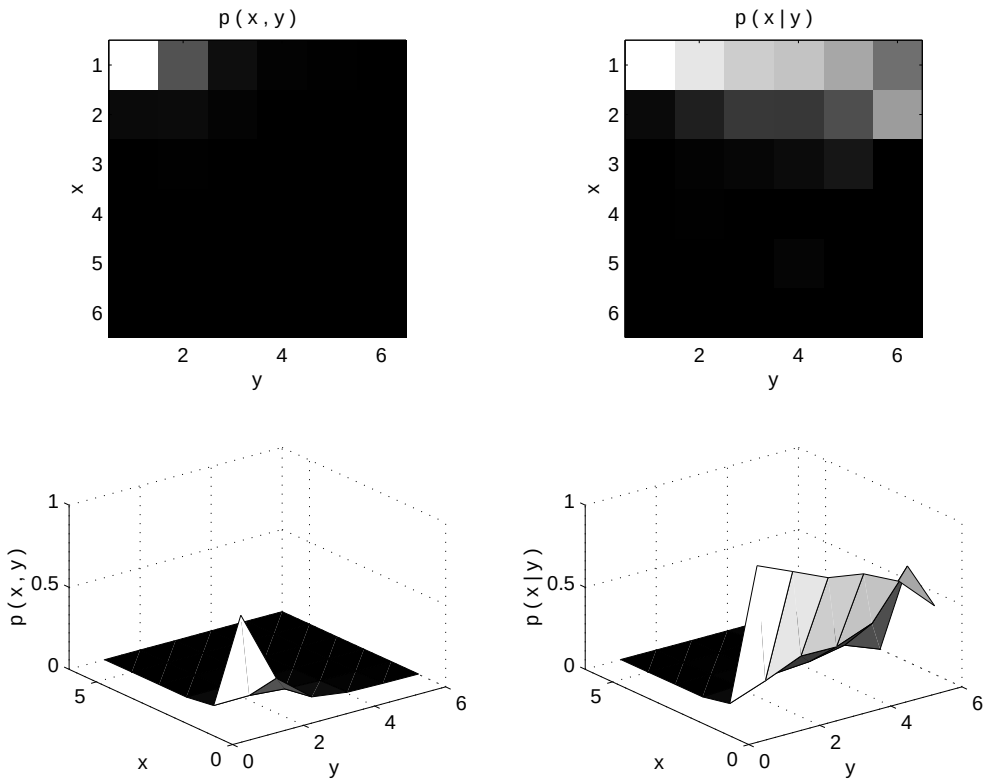

Figure 15: Joint and conditional histograms for subband numbered 43 and its immediate children (binsize=80).

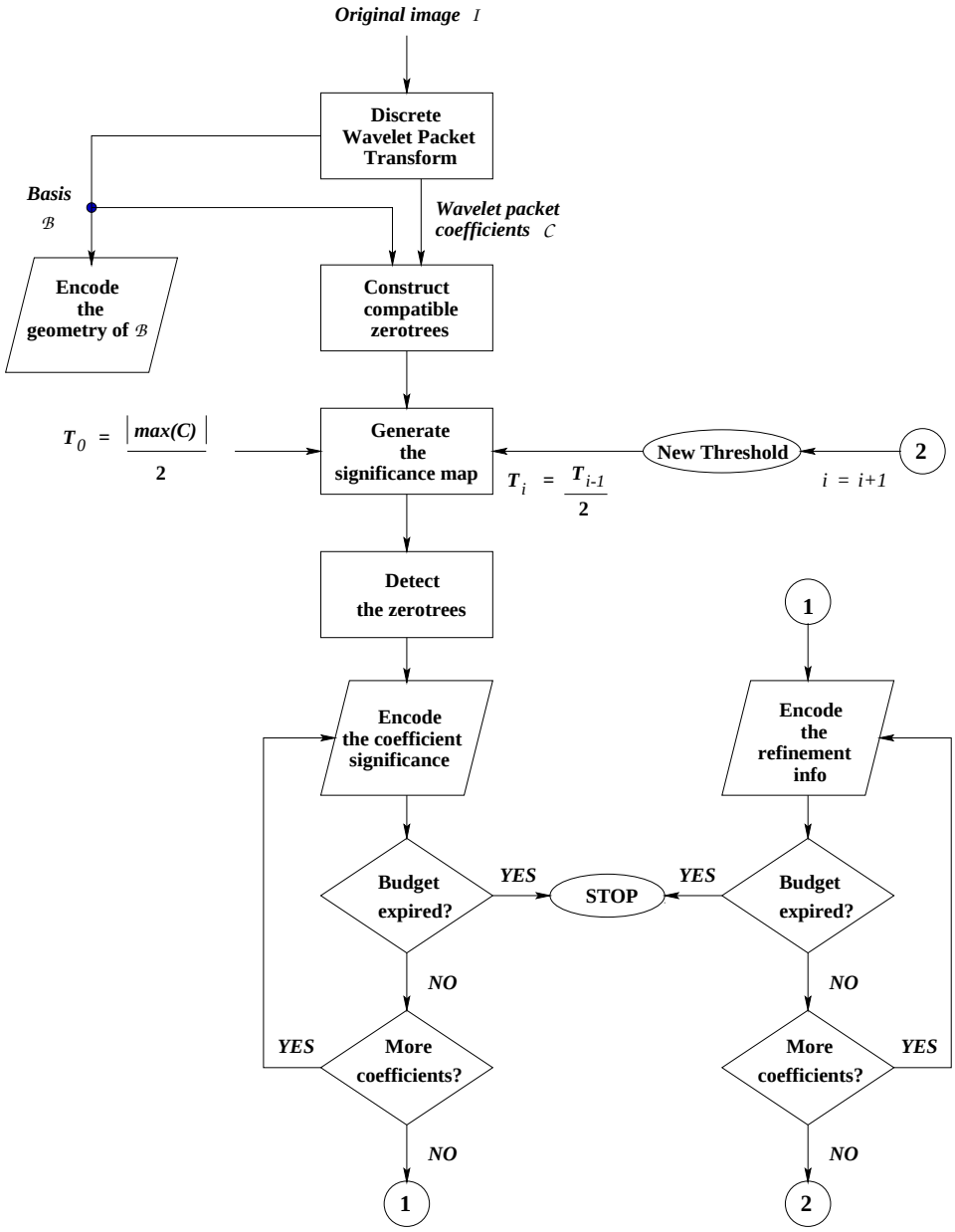

Figure 16: Flowchart of the embedded wavelet packet image coding algorithm employing the compatible zerotree quantization strategy.

ing both wavelet basis and a zerotree friendly wavelet packet basis. The latter of these bases was selected using the actual encoding cost for selecting a basis and then taking simple split/merge decisions on that basis in order to maximize the mutual information $I(X, Y)$. For all the experiments, we used the factorised [8] 9-7 biorthogonal filters [2] for efficiently computing the wavelet packet transform.

Results for the performance of both variations of the CZQ coder - that is, with the wavelet basis (CZQ-Wave) and with the wavelet packet basis (CZQ-WP) - and state-of-the-art SPIHT coder for both the test images (*Barbara* and *Fingerprints*) are presented in Table 1. The measure used to describe the performance of each coder is the peak signal to noise ratio (PSNR) given by

$$PSNR = 20 \log_{10} \frac{255}{\|\mathbf{I} - \mathbf{I}_d\|_2}$$

where $\mathbf{I}$ and $\mathbf{I}_d$ denote the original and the decoded images respectively. Although it is well known that PSNR is not a representative measure of the performance from a perceptual quality viewpoint, it is still widely used for comparing the coding performances in terms of quantitative distortion. The performance difference between SPIHT and CZQ-Wave is due to the following reason. We used a simple first-order adaptive arithmetic coder of [16] for entropy coding of the zerotree quantized codewords and the significance information, as opposed to order-3 arithmetic coders used in both SPIHT and FWP [8].

While being capable of progressively reconstructing the encoded image and being relatively faster - by a factor ranging from two to four - than bitplane coding of the FWP, the CZQ-WP performs comparably well. The coding gain achieved by it, approximately 1dB for *Barbara* and almost 0.5dB for *Fingerprints*, on top of CZQ-Wave verifies the validity of compatible zerotree hypothesis for wavelet packets. Figures 18 and 20 show the geometry of wavelet packet basis selected for *Barbara* and *Fingerprints* images respectively. A closer look at the reconstructed images by CZQ-WP and SPIHT at 0.25 bits per pixel (bpp) reveals that CZQ-WP yields better visual quality than SPIHT. Note, for instance, the quality of a

portion (table cloth) of the reconstructed *Barbara* image encoded by CZQ-WP and SPIHT as shown in Figure 17, and the quality of a portion (central spiral) of the reconstructed *Fingerprints* image encoded by CZQ-WP and SPIHT as shown in Figure 19.

It is worth noting, however, that the effectiveness of zerotree quantization depends strongly upon the scale-invariance of edges among subbands of similar global orientation. We also believe that the so-called *best basis* is optimal only for a given cost function. This function should involve both rate and distortion caused due to the quantization framework being used. Our future work aims to look at employing higher-order contexts for wavelet packet subbands arranged in the compatible zerotree order, and the introduction of a modified cost function which can take into account both distortion and the encoding cost of zerotree quantization.

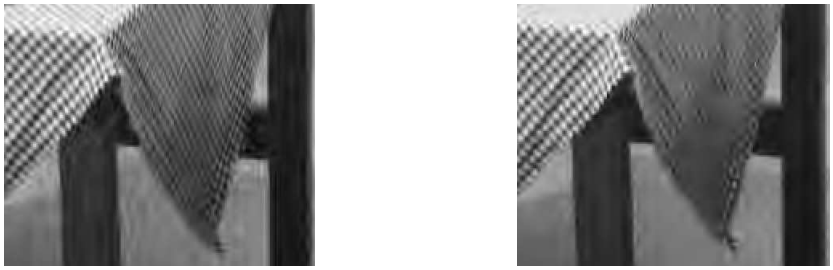

(a) (b)

Figure 17: Portion of *Barbara* (table cloth) encoded at 0.25 bpp by (*a*) CZQ-WP and (*b*) SPIHT.

Appendices

A Algorithm (Generating the Compatible Zerotrees)

1. *Create raw compatible zerotrees.*

   a) For each family of subbands $\mathcal{F} \in \{\mathcal{H},\mathcal{V},\mathcal{D}\}$, create a compatible zerotree using rules *a)*, *b)*, and *c)* of Section 3.2.

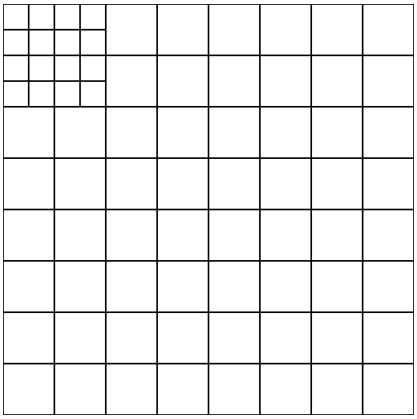

Figure 18: Wavelet packet basis selected for the 512×512 *Barbara* image.

Image	Rate (bpp)	Ratio (:1)	CZQ-Wave	CZQ-WP	SPIHT
Barbara	0.25	32:1	27.12	28.12	27.58
	0.50	16:1	30.28	31.60	31.39
	1.00	8:1	35.14	36.15	36.41
Fingerprints	0.25	32:1	26.53	27.07	27.12
	0.50	16:1	30.65	31.15	31.27
	1.00	8:1	35.24	35.82	36.01

Table 1: Coding results for standard images with texture - *Barbara* and *Fingerprints*.

(a) (b)

Figure 19: Portion of *Fingerprints* (central spiral) encoded at 0.25 bpp by (*a*) CZQ-WP and (*b*) SPIHT.

b) Establish a link between all the three compatible zerotrees generated in step *a)* and the node R representing the lowest frequency subband so that the node R now represents the whole raw compatible zerotree structure.

2. *Resolve the parenting conflicts, if any.*

a) Traverse the whole raw compatible zerotree generated in step 1 to find out two sets of nodes P and C (where $\mid P \mid = \mid C \mid = k$) such that: for all $i = 1, 2, \ldots, k$, P_i - the ith element of P - is the parent node of C_i - the ith element of C - and P_i is at a finer scale than C_i. If $k = 0$, then stop.

b) For $i = 1, 2, \ldots, k$, find out a compatible ancestor node A_i to C_i which is at the same scale or at a coarser scale than C_i itself.

c) For $i = 1, 2, \ldots, k$, delete the link between P_i and C_i and establish a new link between A_i and C_i.

References

[1] R.W. Buccigrossi and E.P. Simoncelli, *Image compression via joint statistical characterization in the wavelet domain*, IEEE Transactions on Image

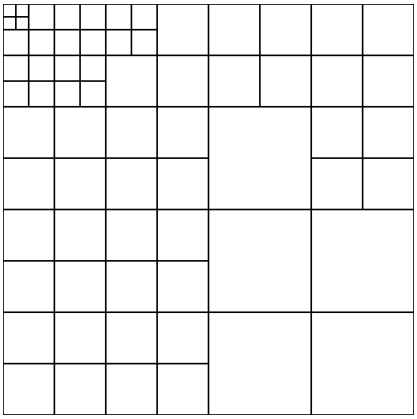

Figure 20: Wavelet packet basis selected for the 512×512 *Fingerprints* image.

Processing (1999), to appear.

[2] A. Cohen, I. Daubechies, and J. Feauveau, *Bi-orthogonal bases of compactly supported wavelets*, Comm. Pure Appl. Math. **45** (1992), 485–560.

[3] R.R. Coifman and Y. Meyer, *Size properties of wavelet packets*, Wavelets and their Applications (Ruskai et al, ed.), Jones and Bartlett, 1992, pp. 125–150.

[4] R.R. Coifman and M.V. Wickerhauser, *Entropy-based algorithms for best basis selection*, IEEE Trans. on Information Theory **38** (1992), no. 2, 713–718.

[5] Thomas M. Cover and Joy A. Thomas, *Elements of informatin theory*, John Wiley & Sons, Inc., 1991.

[6] M. Effros, *Zerotree design for image compression: Toward weighted universal zerotree coding*, IEEE Intl. Conf. on Image Processing, November 1997.

[7] A.S. Lewis and G. Knowles, *Image compression using the 2-D wavelet transform*, IEEE Trans. on Image Processing **1, 2** (1992), 244–250.

[8] F.G. Meyer, A.Z. Averbuch, and J-O. Strömberg, *Fast adaptive wavelet packet image compression*, submitted to IEEE Trans. on Image Processing, April 1998.

[9] F.G. Meyer, A.Z. Averbuch, J-O. Strömberg, and R.R. Coifman, *Multi-layered image representation: Application to image compression*, International Conference on Image Processing, ICIP'98, Chicago, October 4-7, 1998, 1998.

[10] W. Pennebaker and J. Mitchell, *JPEG Still Image Data Compression Standard*, Van Nostrand Reinhold, 1992.

[11] Nasir M. Rajpoot and Roland G. Wilson, *Progressive image coding using augmented zerotrees of wavelet coefficients*, Technical Report CS-RR-350, Dept. of Computer Science, University of Warwick, UK (1998).

[12] K. Ramchandran and M. Vetterli, *Best wavelet packet bases in a rate-distortion sense*, IEEE Trans. on Image Processing (1993), 160–175.

[13] A. Said and W.A. Pearlman, *A new fast and efficient image codec based on set partioning in hierarchical trees*, IEEE Trans.on Circ.& Sys. for Video Tech. **6** (1996), 243–250.

[14] J.M. Shapiro, *Embedded image coding using zerotrees of wavelet coefficients*, IEEE Trans. on Signal Processing (1993), 3445–3462.

[15] R.G. Wilson, A.D. Calway, and R.S. Pearson, *A generalized wavelet transform for fourier analysis: The multiresolution fourier transform and its applications to image and audio signal analysis*, IEEE Trans. on Image Processing **38,2** (1992), 674–690.

[16] I.H. Witten, R.M. Neal, and J.G. Cleary, *Arithmetic coding for data compression*, Communications of the ACM **30,6** (1987), 520–540.

[17] Xiaolin Wu, *High-order context modeling and embedded conditional entropy coding of wavelet coefficients for image compression*, submitted, 1997.

[18] Z. Xiong, O. Guleryuz, and M.T. Orchard, *Embedded image coding based on DCT*, VCIP'97, San Jose, CA, Feb. 1997.

[19] Z. Xiong, K. Ramchandran, and M.T. Orchard, *Wavelet packet image coding using space-frequency quantization*, IEEE Trans. on Image Processing **7, N. 6** (1998), 892–898.